



HAL
open science

Minimizing the Bondline Thermal Resistance in Thermal Interface Materials Without Affecting Reliability

J. A. Emerson, M. J. Rightley, J.A. Galloway, D. F. Rae, Dale. L. Huber, Eric J. Cotts

► To cite this version:

J. A. Emerson, M. J. Rightley, J.A. Galloway, D. F. Rae, Dale. L. Huber, et al.. Minimizing the Bondline Thermal Resistance in Thermal Interface Materials Without Affecting Reliability. THERMINIC 2005, Sep 2005, Belgirate, Lago Maggiore, Italy. pp.106-111. hal-00189460

HAL Id: hal-00189460

<https://hal.science/hal-00189460>

Submitted on 21 Nov 2007

HAL is a multi-disciplinary open access archive for the deposit and dissemination of scientific research documents, whether they are published or not. The documents may come from teaching and research institutions in France or abroad, or from public or private research centers.

L'archive ouverte pluridisciplinaire **HAL**, est destinée au dépôt et à la diffusion de documents scientifiques de niveau recherche, publiés ou non, émanant des établissements d'enseignement et de recherche français ou étrangers, des laboratoires publics ou privés.

MINIMIZING THE BONDLINE THERMAL RESISTANCE IN THERMAL INTERFACE MATERIALS WITHOUT AFFECTING RELIABILITY*

John A. Emerson¹, Michael J. Rightley¹, Jeffrey A. Galloway¹, David F. Rae^{1,2}, Dale L. Huber¹, and Eric J. Cotts²

¹Sandia National Laboratories
Albuquerque, NM 87185-1245

²Binghamton University
Harpur College of Arts and Sciences
Department of Physics
Binghamton, NY 13902

ABSTRACT

As electronic assemblies become more compact, with increased processing bandwidth and higher energy fluxes, thermal management is limiting several critical applications. The major technology limitation is the nonmetallic joining of devices to heat sinks using existing commercial thermal interface materials (TIMs). The present study starts a systematic study of the coupled interactions between materials formulation, manufacturing process, and thermal performance. Thermal bondlines were fabricated under controlled conditions with commercially available TIMs and a nanoparticle-modified epoxy. Force measurements during bondline fabrication provided information about the flow process. Thermal performance of the bondlines was evaluated with laser flash thermal diffusivity measurements. Relationships between flow parameters, final bondline microstructure, and bondline thermal resistance are discussed from the standpoint of reliability and performance.

1. INTRODUCTION

The lack of substantial improvements in thermal interface materials (TIMs) has hindered the heat transport through bondlines, such as at the interfaces between chips and heat spreaders. Although this problem is known [1], a material system solution has been not found. The failure of the interfacial region of the TIMs to have conductivity equivalent to the bulk is centered on three issues: 1) conductive particle depletion layer because of fluid flow phenomena, 2) lack of understanding for the phonon transport using models such as subgrid physics, and 3) conductive nanoparticle inclusions. Thus the next generation TIM requires a sophisticated understanding of material and surface sciences, heat transport at nanoscale lengths, and the manufacturing processes used in packaging of microelectronics and other target applications. We have confirmed the observation that the interfacial versus bulk, thermal resistance is the major loss mechanism and normally accounts for an order of magnitude loss in conductivity per

equivalent thickness [2]. We present our first findings [3] showing the relationships between flow parameters, final bondline microstructure, and bondline thermal resistance with the tradeoffs between material systems, manufacturability (processing), and reliability.

2. BACKGROUND

Prior to cure, epoxy based TIMs are concentrated suspensions of thermal conductive filler particles in a matrix fluid comprising epoxy component - curatives, surface modifiers, conductivity enhancers, and rheology modifiers or solvents. For common TIM materials, filler volume fractions typically range from 20 to 50% w/w. Under squeeze flow, paste-like suspensions deviate from the expected behavior of continuous fluids, with phase separation observed at low squeeze rates [4-9]. The matrix resins are found to flow faster than the filler particles, resulting in filtration and separation. Chaari et al. [4] proposed that this behavior scales with the Peclet number (Pe). Pe may be expressed as [5]:

$$Pe = \frac{\tau_w}{\tau_s} \quad (1)$$

where τ_w is the characteristic time for fluid filtration through the porous media and τ_s corresponds to the characteristic time for deformation of the concentrated suspension. When $Pe < 1$, filtration effects become significant [4]. As shown in reference [9]:

$$Pe = \frac{\mu_w U^{1-m} h^{m+1}}{Ak} \quad (2)$$

where μ_w is the matrix viscosity, U is the squeeze rate, m is the shear thinning index of the paste [9] (quite different from the usual definition [9]), h is the instantaneous gap, A is the consistency or effective viscosity of the paste, and k is the permeability. The factor, U , based upon the degree of void volume fraction and is strongly dependent upon particle size and volume fraction [5]. Thus, at low squeeze rates

and/or small gaps ($Pe < 1$), separation of filler particles and the matrix is expected.

The critical squeeze rate (minimum squeeze rate before the onset of filtration), U_c , occurs when $Pe = 1$ [5]:

$$U_c = \left(\frac{Ak}{\mu_w h^{m+1}} \right)^{1/1-m} \quad (3)$$

As gap widths decrease, faster flow speeds are required to avoid particle/matrix separation.

When $Pe > 1$ and squeeze rate are held constant, the squeeze force varies with the plate separation raised to a constant power [5]. For lower values of Pe , deviations from this dependence are observed. The measurement of force versus plate separation for fixed squeeze rates can be related to the nature of the flow of dense suspensions in squeeze geometries. By knowing the relationship between flow conditions, thermal bondline microstructure, and conductance, improvement in thermal conductivity and component reliability can be addressed.

3. EXPERIMENTAL

Two commercial TIMs (T1 and T2) and a third material (T3) consisting the addition of 5% w/w Ag nanoparticle to the T1 were studied. Table 1 summarizes the bulk properties of the materials. The density, ρ , was determined from the masses and geometries. The heat capacity, C_p , was determined from DSC measurements. The thermal diffusivity, α , was determined from laser flash diffusivity measurements. Thermal conductivity, λ , was calculated from:

$$\lambda = \alpha \cdot \rho \cdot C_p \quad (4)$$

The value, λ_{vendor} , was obtained from vendor literature. Their values are optimistic compared to our measurements.

Thermograms are collected by a spring loaded thermocouple measuring the transient response of the sample back face temperature. The rear face temperature profile is fitted to the heat

ID	Material	ρ (g/cm ³)	C _p (J/gK)	α (cm ² /s)	λ (W/mK)	λ_{vendor} (W/mK)
Epoxy	Unfilled epoxy	1.02	1.3	0.0013	0.2	-
T1	Ag flake filled TIM	3.13	0.51	0.0113	1.8	29
T2	Ag flake filled TIM	2.84	0.45	0.0830	11	17
T3	5% Nanocomposite	2.76	0.61	0.0051	0.6	-

Table 1. Thermal and Physical Properties of Bulk Samples

transport equation for the specific sample geometry. The analysis for bulk samples and multilayer samples, T1 and T3, consider heat losses from the faces using a non-linear least squares method. Furthermore, T1 and T3 multilayer samples were analyzed in detail with a new numerical method being developed by Anter Corporation. This led to significant improvements over the alternative models including the consideration of front and back faces heat losses and the evaluation of the middle layer as a thermal contact resistance between the two substrates. For the T2 multilayer samples the method of Lee [10] was deployed.

Bulk samples of the TIM material for laser flash analysis were prepared by dispensing into 12.7 mm diameter disk shaped molds and curing following the manufacturer's recommendation. After cure they were machined to a thickness of approximately 1 mm and the front and back surfaces were finished with 600 grit SiC paper. Prior to testing, a thin-film coating of Au/Pd and an overcoat of graphite was added to provide an optical coupling to the laser beam.

To evaluate the bondline formation process and the thermal performance of the TIMs, Al, 6061 T6, substrates (arithmetic roughness of $\sim 1 \mu\text{m}$) were bonded together with a thin layer of TIM. To control the bondline assembly a TA Instruments ARES Rheometer with vacuum ports secured the substrates after alignment and during the squeeze assembly. After zeroing the gap between substrates on the rheometer, the lower substrate was removed and a volume of

TIM material was dispensed onto the center of the substrate while the mass was monitored with a microbalance. Target masses were established based upon the density of the material used and the final bondline thickness. Using an alignment tool, the lower substrate was relocated back on the fixture.

Parameters controlled during the squeeze included the target bondline thickness and squeeze rate. The maximum load of the ARES rheometer was 2 kg. After the squeeze, the nominal final thickness was maintained for five minutes before the sample was removed and cured following the manufacturer's guidelines.

4. RESULTS AND DISCUSSION

Values of thermal conductivity for the bulk TIM samples, as determined from thermal diffusivity measurements, are shown in Table 1. Each value for thermal diffusivity and conductivity is the average of separate measurements made on three different samples. The values obtained for an unfilled epoxy sample is included for comparison.

Measurements of normal force (F) as a function of instantaneous gap width (h) as measured in the rheometer, at constant squeeze rate, for T1 multilayer samples are presented in Figure 1. For faster constant squeeze rates ($U > 1 \mu\text{m/s}$) a simple power law dependence of force on the nominal gap width was observed. At small gap widths, deviation in the direction of lower forces is shown for these squeeze rates corresponding to the squeeze out of material from the edges of

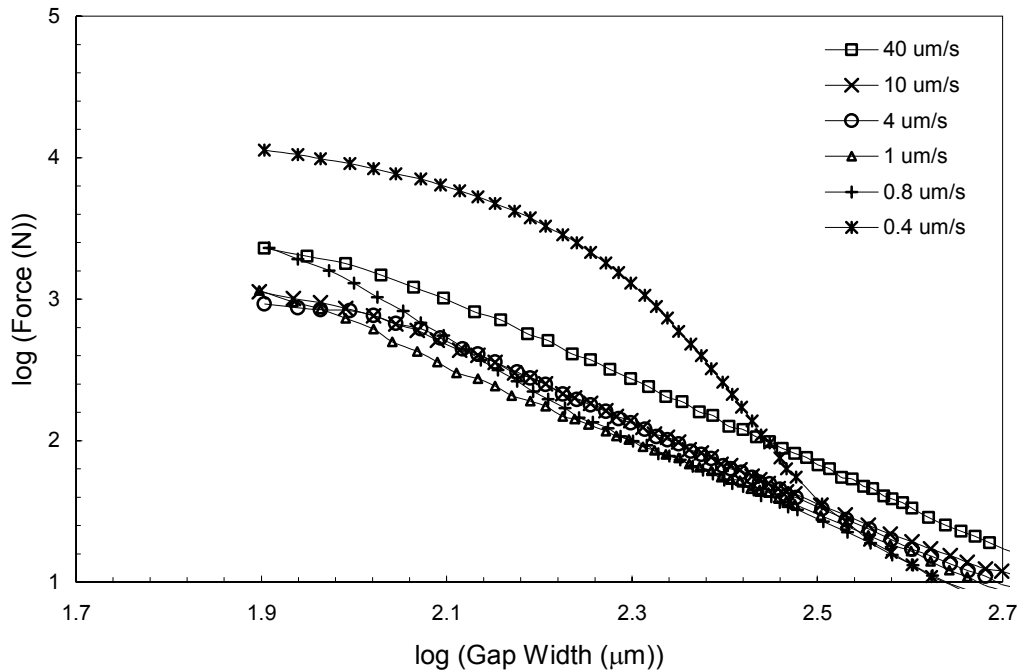


Figure 1. Log Normal Force vs. Log Instantaneous Nominal Gap Width for T1, Several Squeeze Rates (U) Are Displayed.

the gap. For slower speeds, similar simple power law dependence is observed for higher gap widths, but as gap width decreased a distinct deviation from the curve in the direction of higher forces was found. Such systematic variation in flow behavior with squeeze rate is consistent with a dependence of flow behavior on Peclet number (Eq 2). Former work has identified a simple power law dependence of force on plate separation with the flow of an essentially homogeneous fluid. For squeeze flows [8] at a given rate, the separation of particles and suspension fluid results in deviations from a simple power law dependence of force on plate separation. At lower plate separations and speeds a boundary between the two regimes is seen on a force versus plate separation plot [9]. The deviations from simple

power law dependence for higher forces at low values of plate separation result in filtration and jamming of the particles between the substrates, as shown in Figure 1. The observed variations in packing fraction for lower squeeze rates indicate a corresponding variation in thermal conductance across the bondline. These results indicate that force versus gap width curves can be indicative of important spatial variations in thermal bondline resistance. An expected result of such heterogeneity over the bondline is hot spots on an active component.

The bondline thermal resistance and bondline thickness is shown in Figure 2, where bondline thickness was evaluated by averaging the thickness of the sample in 4 locations. The thermal resistance of the bondline depends

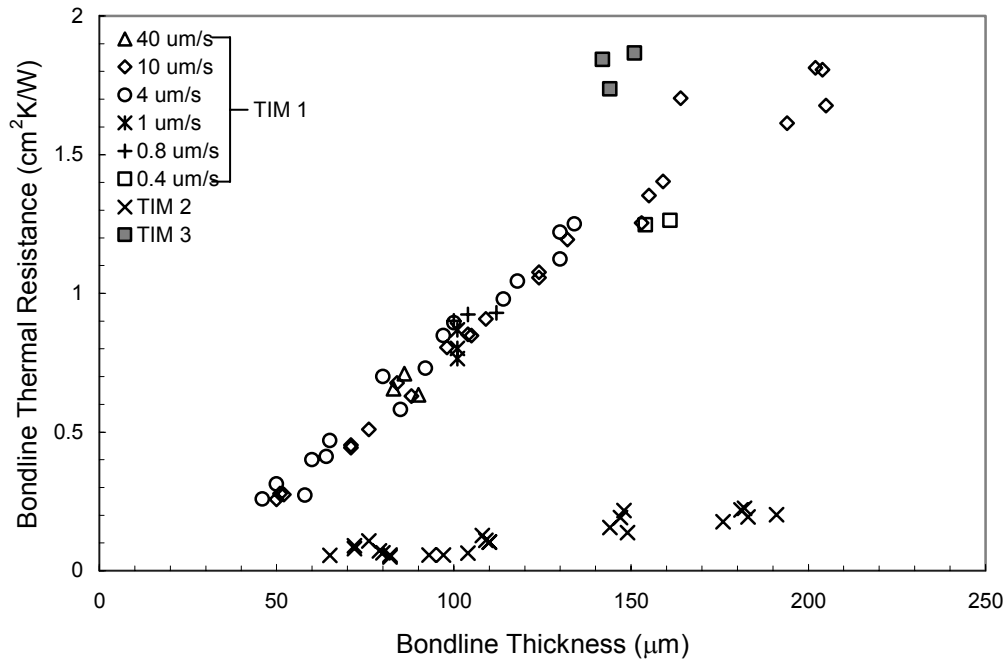


Figure 2. Thermal Resistance Versus Bondline Thickness for Multilayer Samples; T1 Used Different Squeeze Rates for Bondline Formation; T2 and T3, the Rate - 10 µm/s.

on thickness for the T1 multilayer samples of bondline thickness of less than 100µm. Linear fit results in a negative intercept. The value of the intercept is often interpreted as an interface resistance; however, this value is negative. The negative intercept is observed because the thermal conductivity of the material increases as the filler redistributes between the plates during the bondline assembly [11,12].

With the addition of the 5% silver nanoparticles to the bondline, no enhancement was achieved over the use of the base T1. The results of our preliminary nanocomposite work show a decrease in the bulk thermal conductivity over T1 because of several factors. The first is voiding observed in the bulk cross-sectioned laser flash diffusivity sample. Voids were likely entrapped during the casting process because of the increase in viscosity. Second, the alkylthiol coating on the nanoparticle effectively reduces the relative amount of silver in the epoxy as it comprised 50% of the nanoparticle mass. This

results in a reduction of the silver content from approximately 70 wt% to 69%. Third, Fan et al. showed that introduction of nanoparticles created additional thermal interfaces between the micron-scale silver plates in similarly filled epoxies thus decreasing the efficiency of thermal transport and decreasing the bulk thermal conductivity [13].

Thus several factors come into play when increasing the Ag loading via nanoparticle or standard Ag particles. With nanoparticles, the material processing becomes difficult leaving voids. The voids lower thermal conductivity as well as the bond strength. In the case of high filler densities the bond strength is greatly reduced giving very poor adhesion. This poor adhesive and cohesive strength greatly lowers the reliability of the device to the point of major concern.

5. SUMMARY

In this work, we report on formation of the final bondline microstructure by varying the rate and resultant pressure of bondline formation. The observed behavior scales with the Peclet number (Pe), i.e., advective and diffusive flow components or filtration and separation. At $Pe < 1$, filtration is resulting in slightly improved thermal conductivity (as measured by laser flash diffusivity), however, at the loss of reliability because of poor adhesion. Also, thermal conductivity of nanoparticle-modified TIMs did not increase because of the alkanethiols that self-assemble during synthesis form a monolayer on the silver surfaces that's acts as a thermal insulating layer.

Bondline assembly characteristics and bondline microstructure are coupled in improving bondline thermal conductance. Another important factor to consider is the decrease in bond strength resulting in serious reliability issues when attempting to increase the filler density in the bondline.

6. ACKNOWLEDGEMENTS

Thanks to Prof. Lawrence P. Lehman of the Physics Department at Binghamton University for the image analysis. Marc-Antoine Thermitus, Anter Corporation, provided the data analysis package for the laser flash diffusivity experiments.

7. REFERENCES

* Sandia is a multiprogram laboratory operated by Sandia Corporation, a Lockheed Martin Company, for the United States Department of Energy's National Nuclear Security Administration under Contract DE-AC04-94AL85000.

[1] Ravi Mahajan, Raj Nair, Vijay Wakharkar, Johanna Swan, John Tang, and Gilroy Vandentop, "Emerging Directions For Packaging Technologies," Intel Technology Journal, 6(2), pp. 62-75, 2000.

[2] John Emerson, Jeffrey Galloway, David Rae, and Michael Rightley, "Thermal Interface Materials

Advancements for "Beating the Heat" in Microelectronics," Society for the Advancement of Material and Process Engineering, *Technical Conference Proc.: Advancing Materials in the Global Economy—Applications, Emerging Markets and Evolving Technologies*, Long Beach, CA, May 1–5, 2005.

[3] An extended version of this manuscript will be published in *Thermal Conductivity 28 – Proceedings of the Twenty Eighth International Conference 2005*.

[4] F. Chaari, G. Racineux, A. Poitou, and M. Chaouche, "Rheological Behavior of Sewage Sludge and Strain-Induced Dewatering," *Rheol. Acta.*, 42(3), pp. 273-279, 2003.

[5] J. Collomb, F. Chaari, and M. Chaouche, "Squeeze Flow of Concentrated Suspensions of Spheres in Newtonian and Shear-Thinning Fluids," *J. Rheology.*, 48(2), pp. 405-416, 2004.

[6] A. Poitou, and G. Racineux, "A Squeezing Experiment Showing Binder Migration in Concentrated Suspensions," *J. Rheology.* 45(3), pp. 609-625, 2001.

[7] N. Delhaye, A. Poitou, and M. Chaouche, "Squeeze Flow of Highly Concentrated Suspensions of Spheres," *J. Non-Newtonian Fluid Mech.*, 94(1), pp.67-74, 2000.

[8] F. Kolenda, P. Retana, G. Racineux, and A. Poitou, "Identification of Rheological Parameters by the Squeezing Test," *Powder Technol.*, 130(1), pp. 56-62, 2003.

[9] J. D. Sherwood, "Liquid–Solid Relative Motion during Squeeze Flow of Pastes," *J. Non-Newtonian Fluid Mech.*, 104:1-32, 2002.

[10] H.J. Lee, "Thermal Diffusivity in Layered and Dispersed Composites," Ph.D. dissertation, School of Mech. Eng., Purdue Univ., West Lafayette, 1975.

[11] R.C. Campbell, S.E. Smith, and R.L. Dietz, "Laser Flash Diffusivity Measurements of Filled Adhesive Effective Thermal Conductivity and Contact Resistance Using Multilayer Methods" in *Thermal Conductivity 25*, C. Uher and D. Morelli, eds: Lancaster Technomic Publishing Company, Inc., pp.191-202, 2000.

[12] R.C. Campbell, S.E. Smith, and R.L. Dietz, "Measurements of Adhesive Bondline Effective Thermal Conductivity and Thermal Resistance Using the Laser Flash Method," in *Fifteenth Annual IEEE Semiconductor Thermal Measurement and Management Symposium*, San Diego, CA: IEEE, pp.83-97, 1999.

[13] L. Fan, B. Su, J. Qu, and C.P. Wong, "Electrical and Thermal Conductivities of Polymer Composites Containing Nano-Sized Particles," in *54th Electronic Components and Technology Conference*, Las Vegas, NV: IEEE, pp. 148-154, 2004.